Bioresource Technology 103 (2012) 64–70

Contents lists available at SciVerse ScienceDirect

Bioresource Technology

journal homepage: www.elsevier.com/locate/biortech

Prediction of removal efficiency of Lanaset Red G on walnut husk using artificial neural network model

Abuzer Çelekli [a,*], Sevil Sungur Birecikligil [b], Faruk Geyik [c], Hüseyin Bozkurt [d]

[a] Department of Biology, Faculty of Art and Science, University of Gaziantep, 27310 Gaziantep, Turkey
[b] Department of Biology, Faculty of Art and Science, University of Nevşehir, 50300 Nevşehir, Turkey
[c] Department of Industrial Engineering, Faculty of Engineering, University of Gaziantep, 27310 Gaziantep, Turkey
[d] Department of Food Engineering, Faculty of Engineering, University of Gaziantep, 27310 Gaziantep, Turkey

ARTICLE INFO

Article history:
Received 2 August 2011
Received in revised form 20 September 2011
Accepted 24 September 2011
Available online 1 October 2011

Keywords:
Adsorption
ANN
Walnut husk
Lanaset Red G
Modeling

ABSTRACT

An artificial neural network (ANN) model was used to predict removal efficiency of Lanaset Red (LR) G on walnut husk (*WH*). This adsorbent was characterized by FTIR-ATR. Effects of particle size, adsorbent dose, initial pH value, dye concentration, and contact time were investigated to optimize sorption process. Operating variables were used as the inputs to the constructed neural network to predict the dye uptake at any time as an output. Commonly used pseudo second-order model was fitted to the experimental data to compare with ANN model. According to error analyses and determination of coefficients, ANN was the more appropriate model to describe this sorption process. Results of ANN indicated that pH was the most efficient parameter (43%), followed by initial dye concentration (40%) for sorption of *LR G* on *WH*.

1. Introduction

Presence of coloring materials with other contaminants in freshwater has become a major environmental problem. They threat Earth because of their adverse effects on all forms of life (WHO, 2000; Rafatullah et al., 2010). Therefore, great attention has been given for removing of dyes from wastewaters during the last few years.

Among various water treatment processes, sorption can be considered as an effective and eco-friendly process to remove color from wastewaters (Srinivasan and Viraraghavan, 2010; Çelekli et al., 2010a). Operating variables such as pH, temperature, dye concentration, contact time, and others affect the sorption process. Insight to sorption behavior, kinetic data should be modeled at the selected optimum operating conditions. In sorption systems, output(s) is\are considered to be closely related to multi-input operating variables.

Artificial neural network (ANN) resembles a data processing (learning) and decision making system of human (Khataee and Kasiri, 2010). As in nature, the network function is determined largely by the connections between elements like human's brain and nerves. ANN consists of simple processing units called neurons. ANN is generally a parallel interconnected structure consisting of input layer of neurons, a number of hidden layers, and output layer. The input layer of neurons acts like a distributor and the inputs are directly transmitted to the hidden layer. The topology of an ANN is determined by the number of its layers, the number of nodes in each layer and the nature of transfer function (Khataee and Kasiri, 2010; Khataee et al., 2011). ANN has been successfully applied by Kumar and Porkodi (2009), Çelekli and Geyik (2011), and Khataee et al. (2011) to predict the sorption of solid–liquid systems and performance of the biological systems. ANN has been used to investigate the relative importance of parameters during sorption kinetics or biodegradation of dyes in the literature (Khataee et al., 2010; Çelekli and Geyik, 2011; Yang et al., 2011). ANN had been applied to describe biosorption of reactive dyes (Dutta et al., 2010), methylene blue (Cavasa et al., 2011), and textile dyes (Balci et al., 2011).

Various agricultural biomasses were used for sorption process to remove unwanted materials from polluted water such as pineapple (Chowdhury et al., 2011a), peanut husk (Song et al., 2011), wheat straw (Xu et al., 2010), rise husk (Chowdhury et al., 2011b), pine cone (Mahmoodi et al., 2011a), coconut husk (Gupta et al., 2010), pistachio husk (Çelekli et al., 2010a), canola hull(Mahmoodi et al., 2010), tamarind hull (Khorramfar et al., 2010; Mahmoodi et al., 2011b), and hazelnut shell (Doğan et al., 2009). For this purpose, walnut shell was used for the removal of chromium (Wang et al., 2009) and the sorption of methylene blue (Yang and Qiu, 2010).

Walnut (*Juglans regia* L.) is one of the widely cultivated fruit tree species in Anatolia and annual walnut production in Turkey

* Corresponding author. Tel.: +90 3423171925; fax: +90.3423601032.
E-mail addresses: celekli.a@gmail.com (A. Çelekli), sevilsungur@hotmail.com (S.S. Birecikligil), fgeyik@gantep.edu.tr (F. Geyik), hbozkurt@gantep.edu.tr (H. Bozkurt).

0960-8524/$ - see front matter © 2011 Elsevier Ltd. All rights reserved.
doi:10.1016/j.biortech.2011.09.106

(172.5 tones) comes after China (503.0 tones) and USA (290.3 tones) (Muradoğlu et al., 2010). Therefore, walnut husk (*WH*) was chosen for this study because of its relatively abundant material. The objective of this study was (i) to investigate adsorption efficiency for removing of Lanaset Red (*LR*) G on *WH* (*J. regia* L.), (ii) to develop three-layer ANN model, and (iii) to perform pseudo second order kinetic model. In order to evaluate the goodness of fitting for comparison of both models, error functions and determination of coefficient were calculated by use of predicted data from these models and experimental data. Effects of particle size, adsorbent dosage, initial pH value, initial dye concentration, and contact time on this sorption were evaluated.

2. Methods

2.1. Adsorbent

Walnut husk (*WH*) was collected from Gaziantep, Turkey. Collected sample was dried in an oven at 80 °C for 24 h, grinded, and sieved as three particles sizes (125–250, 250–500, and >500 μm). Zero point charge (pH_{zpc}) of *WH* was determined by using powder addition method (Kumar and Porkodi, 2007).

Infrared spectrum of unloaded and dye-loaded adsorbents at pH 1 were obtained by use of a Fourier transform infrared equipped with an attenuated total reflection (FTIR–ATR) spectrometer (Perkin–Elmer Spectrum 100 FTIR–ATR Spectrometer).

2.2. Preparation of dye solution

Mixture of azo metal complex dye, *LR G* ($C_{32}H_{21}CrN_{10}O_{11}S{\cdot}2Na$, CAS No.; 70209-87-9, Huntsman, and λ_{max} = 475 nm) was obtained from a local textile company and used without further purification and its structure is given in Fig. 1. Stock dye solution was prepared by dissolving 1 g of dye in 1 L of distilled water. Experimental solutions of desired concentration were obtained by further dilution from the stock solution.

2.3. Sorption studies

Effects of particle size (>500–125 μm), adsorbent dose (0.5–4.0 g L^{-1}), initial pH value (pH_i 1–10), initial dye concentration (50–800 mg L^{-1}), and contact time (0–360 min) on the sorption were investigated. These studies were carried out with in 250 mL conical flask containing 100 mL of the adsorption solution (with desired concentration and pH) and desired adsorbent concentration. Initial pH of each solution was adjusted to desired value with 0.1 M HCl and/or 1.0 M NaOH solutions. These flasks were stirred on the orbital shaker at 150 rpm for 360 min.

During sorption studies, withdrawn samples (0, 5, 10, 15, 30, 45, 60, 90, 120, 150, 180, 210, 240, 270, 300, 330, and 360 min) were centrifuged to precipitate suspended biomass at 5000 rpm for 5 min. The residual *LR G* concentration in the supernatant was analyzed by use of spectrophotometer (Jenway 6305) at 475 nm. Each data point was the mean of two independent sorption studies.

In this study, q_t and q_e show the amount of *LR G* adsorbed on *WH* at time t and at equilibrium (mg g^{-1}) calculated by use of the following equations, respectively.

$$q_t = \frac{(C_o - C_e) \times V}{M} \quad (1)$$

$$q_e = \frac{(C_o - C_e) \times V}{M} \quad (2)$$

where C_o, C_t, and C_e represent the dye concentrations (mg L^{-1}) at initial, at t time, and at equilibrium in the solution, respectively. V is the volume of solution (L), and M is the mass of adsorbent (g L^{-1}).

2.4. Kinetic modeling

2.4.1. Pseudo second-order modeling

Pseudo second-order model was fitted for modeling of *LR G* on the *WH*. The non-linear fitting procedure was performed by use of commercial computer software SigmaPlot version 11 (Systat Sofware, Inc., CA, USA) via the Marquardt–Levenberg algorithm (Çelekli et al., 2011).

2.4.2. Artificial neural network (ANN)

ANN inspired by biological neuron processing can be used to predict the sorption. This multilayered network is a structure consisting of (i) input layer of neuron (independent variables), (ii) a number of hidden layers, and (iii) output layer (dependent variables) (Khataee et al., 2010, 2011; Çelekli and Geyik, 2011).

An ANN was trained to perform a particular (activation) function by adjusting the values of the connections (weights) between elements (neurons) as seen in Fig. 2. The activation function produced the output using a sum weight of each neuron (W_i) and a bias (b_i) that a constant weight of a neuron representing the generalization error. To calculate the weight of a neuron (Eq. (3)) was multiplied by the corresponding weight of the neuron connection and each input coming to that neuron:

$$W_i = \sum_{j=1}^{n} w_{ij} x_j \quad (3)$$

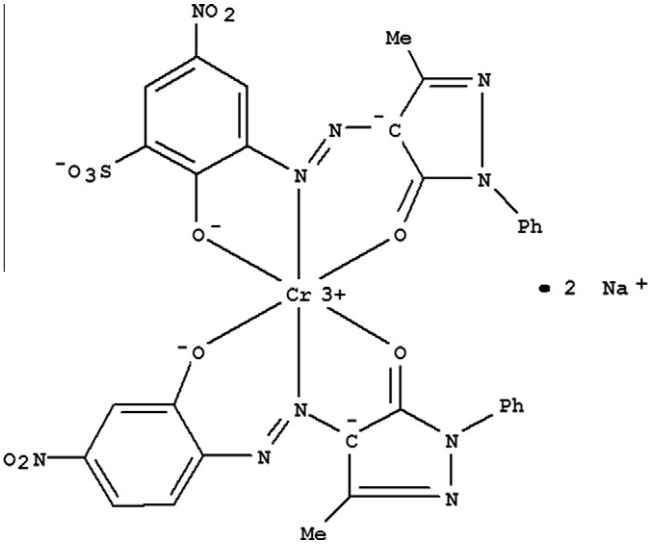

Fig. 1. Chemical structure of Lanaset Red G.

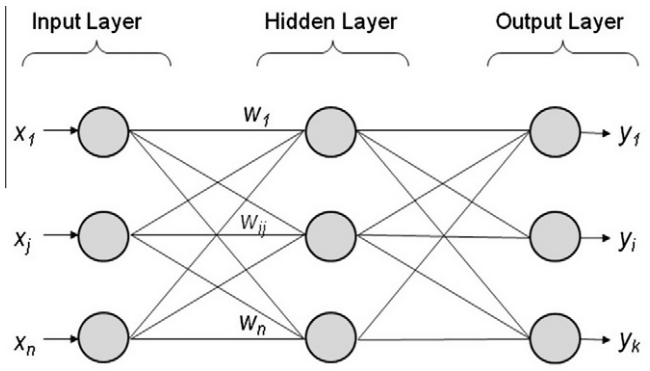

Fig. 2. Architecture of multilayer back propagation neural network.

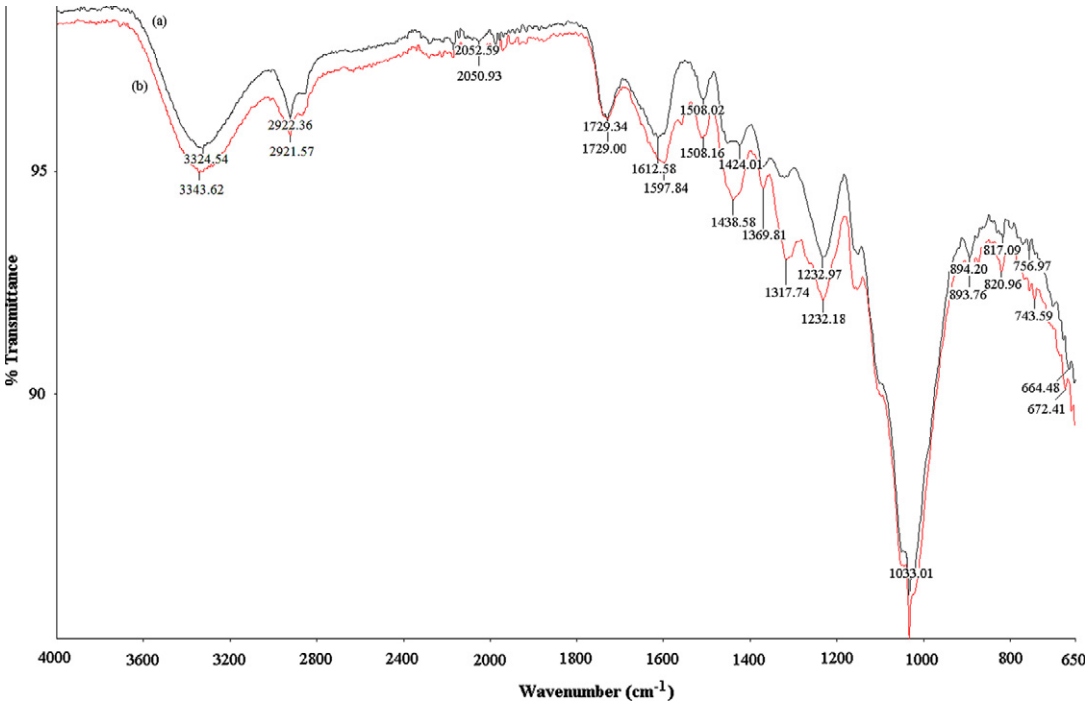

Fig. 3. FTIR spectra of: (a) the nature adsorbent and (b) LR G loaded adsorbent.

where x_j is value of the input j at the input layer and w_{ij} is the corresponding weight of connection between each neuron (j) in input layer and each neuron (i) in hidden layer, and also between hidden and output layers. So an activation function held the final weights between neurons of all network and produced the predicted output by Eq. (4). So an activation function held the final weights between neurons of all network and produced the predicted output by Eq. (4).

$$y_k = f(W_i + b_i) \tag{4}$$

Activation function f may be sigmoidal, linear, radial or other types. Sigmoidal and linear functions are very common especially in back-propagation ANN. Logistic and hyperbolic tangent sigmoid functions are generally used for hidden layer, while linear transfer functions can be used at output layer. Log-sigmoid function is sigmoidal between in 0 and 1, while tan-sigmoid is between in −1 and 1. On the other hand linear transfer function is uniform between in −1 and 1.

In this study, the tan-sigmoid transfer function with back-propagation algorithm at hidden layer and a linear transfer function at output layer transfer functions were used. Tan-sigmoid transfer function is expressed as:

$$f(x) = \frac{1}{1 + \exp(-x)} \tag{5}$$

where $f(x)$ is hidden neuron output. In the study, 408 experimental mean data points were used to feed the ANN structure. The ranges of operating variables were four pH_i values, six initial dye concentrations, and 17 contact time points. The samples were divided into training, validation, and test sets that each of them contains 278, 65, and 65 samples, respectively. All samples were to be scaled into the 0.1–0.9 due to using sigmoid transfer function in the hidden layer.

2.5. Statistical analyses

Analysis of variance (ANOVA) was carried out to determine significant difference as function of operating variables by use of the SPSS version 15.0 (SPSS Inc., Chicago, IL, USA) (Çelekli and Geyik, 2011). This algorithm is used to minimize the sum of square of differences between experimental and predict data. In order to evaluate the goodness of fitting, coefficient of determination (R^2) and the mean squares error (MSE) were carried out between experimental and predicted data from models (Çelekli and Geyik, 2011).

3. Results and discussion

3.1. Characterization of adsorbent

FTIR–ATR spectra of unloaded and *LR G*-loaded adsorbents at pH 1 were obtained and compared to understand interaction between dye and adsorbent.

Several major intense bands, around 3324, 2922, 1729, 1612, 1508, 1424, 1232, 1033, and 894 cm^{-1} were observed in unloaded adsorbent (Fig. 3). The peak at 3324 cm^{-1} could be attributed to —OH and —NH_2 groups (Çelekli et al., 2010b; Yang and Qiu, 2010), while the peak at 2922 cm^{-1} could be assigned to —OH stretching vibrations (Arief et al., 2008). The appearance a band at 1729 cm^{-1} may be related carbonyl (C=O) groups (Yang and Qiu, 2010). The peak at 1612 cm^{-1} could be corresponds to the olefinic C=C stretching vibrations (Yang and Qiu, 2010). The C=C vibrations in aromatic rings cause to the peak of 1508 cm^{-1} and the peak at 1424 may be attributed to —OH and —C—O stretching vibrations (Yang and Qiu, 2010). The peak at 1232 cm^{-1} could be ascribed to the —C—O stretching and groups of —C—O and —C—C groups could be related to the peak of 1033 cm^{-1} (Arief et al., 2008). The sorption peak of 894 cm^{-1} could be attributed to the —C—H out of plane bending vibrations in benzene derivative (Yang and Qiu, 2010).

In the present study, with the loading of *LR G* on the adsorbent shifting of the peaks is seen from 3324, 2922, 1612, 1424, and 894 cm^{-1} (Fig. 3). These are could be due to new bonds formed between the adsorbent and the dye molecules. The FTIR spectrum of adsorbent indicated that *LR G* molecules could be bound in the

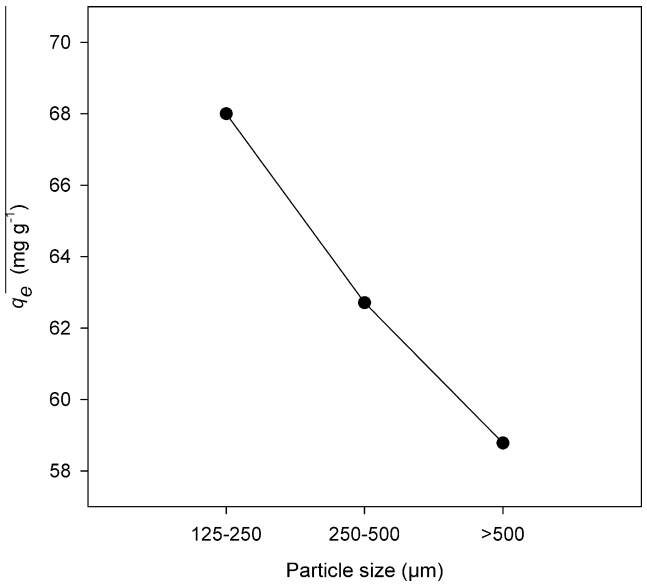

Fig. 4. Effect of particle size on the adsorption of LR G on *WH* at 100 mg L^{-1}.

presence of amine and amide groups, agreement with the findings of Çelekli and Geyik (2011).

3.2. Effect of particle size

In order to evaluate effects of particle size on the sorption process, three particle sizes (125–250, 250–500, and >500 μm) of *WH* were conducted with 100 mg L^{-1} *LR G* solution (Fig. 4). Amount of dye adsorbed increased with decrease in particle size, due to increase in surface area and better accessibility of the pores for dye molecules. Breaking of large particles into smaller ones can also open some tiny sealed channels, which might then become available for the sorption. Similar results have been observed for removing of cyanosine on the coconut husk (Gupta et al., 2010) and the sorption of dyes on the bamboo (Mui et al., 2010). Sufficient better sorption could be achieved at the lower particle size. Hence all further studies were carried out using 125–250 μm particle size of the *WH*.

3.3. Effect of adsorbent dose

Sorption of *LR G* (100 mg L^{-1}) was carried out with four adsorbent doses (0.5, 1.0, 2.0, and 3.0 g L^{-1}). The highest sorption was observed at 1.0 g L^{-1} adsorbent concentration, followed by 0.5 g L^{-1}, whereas the lowest value was measured at 3.0 g L^{-1}. These results could be explained as a consequence of partial overlapping or aggregation of adsorbent at higher biomass concentration, which cause to decrease in effective surface area for the sorption process. These are in agreement with result of Gao et al. (2010), in which using granular sludge for the sorption of acid Yellow 17 and the sorption of Reactive Red 194 and Direct Blue 53 on cupuassu shell (Cardoso et al., 2011). Therefore, the adsorbent dose of 1.0 g L^{-1} was selected for the further studies.

3.4. Effect of initial pH (pH$_i$) value

Solution's pH is an important environmental driving factor in the sorption process by influencing functional groups on adsorbent surface and also solubility of dyes (Rafatullah et al., 2010).

Change in initial pH (pH$_i$) values from 1 to 10 strongly affected ($p < 0.01$) the sorption of *LR G* (Fig. 5a). Amount of dye adsorbed was found to be the lowest at pH$_i$ value of 10, whereas the highest at pH$_i$ value of 1. Determination of zero point charge (pH$_{zpc}$) of adsorbent is an important parameter for understanding of sorption mechanism. The pH$_{zpc}$ of *WH* was found to be 6.1 (Fig. 5b). The adsorbent surface could be become positively charged at lower pH values than pH$_{zpc}$, which favored the sorption of *LR G* due to electrostatic attraction. Limitation of the sorption capacity of dye molecules increased with increase in electrostatic repulsion at higher pH$_i$. This is an agreement with previous studies (Gupta et al., 2010; Çelekli et al., 2011). Consequently, positively charged functional groups could exert strong electrostatic attractions with anionic dye molecules, as the increase in sorption capacity of *WH* at pH$_i$ 1.

3.5. Effect of contact time and initial dye concentration

In this study, rapid sorption of *LR G* on *WH* was observed during the first 80 min of contact time. After then, removal rate of the dye molecules gradually decreased until equilibrium. The rapid sorption could be consequence of abundancy of functional groups on the adsorbent surface in the initial stages of contact time.

Effect of initial dye concentration (C_o = 50–800 mg L^{-1}) on the sorption of *LR G* on *WH* was investigated at aforementioned optimum conditions (M = 1 g L^{-1} and the particle size of 125–250 μm). Results indicated that the *LR G* uptake strongly increased ($p < 0.01$) with increasing initial dye concentration. This could be consequence of increase in the driving force for mass transfer, in agreement with

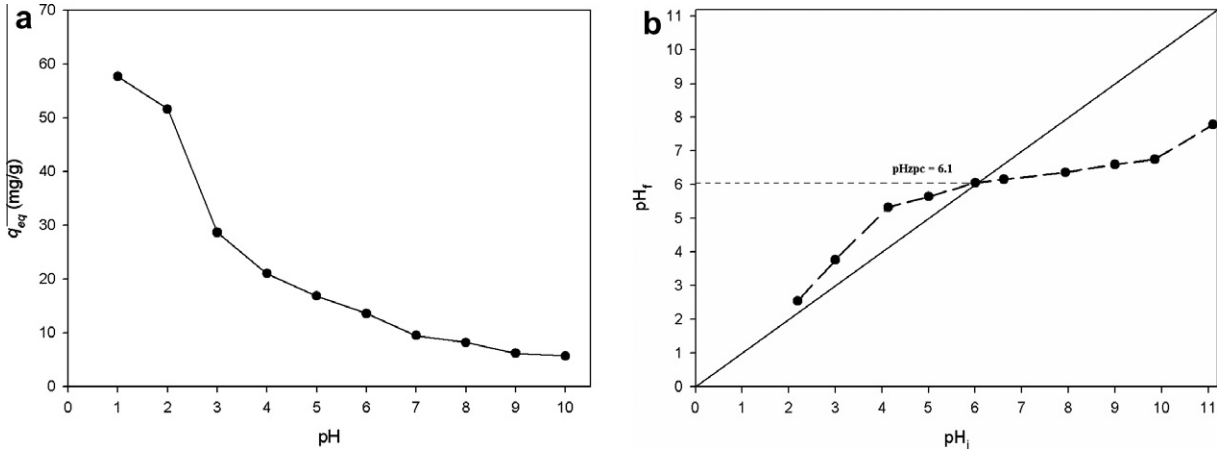

Fig. 5. (a) Effects of initial pH values on the sorption of *LR G* on *WH* and (b) pH$_{zpc}$ of *WH*.

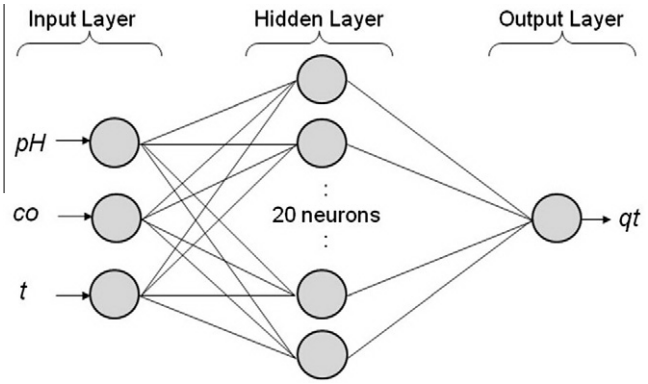

Fig. 6. ANN optimized structure (pH_i = 1–4, C_o = 50–800 mg L^{-1}, and t = 0–360 min).

results of previous studies (Chowdhury and Saha, 2010; Çelekli et al., 2010a; Khataee et al., 2010; Wang et al., 2010).

3.6. Kinetic modeling

Artificial neural networks (ANN) and pseudo second-order kinetic model were used to investigate the sorption of *LR G* on *WH*.

Pseudo second-order kinetic (Ho and McKay, 1999) is one of the most widely used kinetic models to predict the relationship between q_{exp} and $q_{predict}$. This model was found to be successful in representing the kinetics of several sorption systems (Plazinski et al., 2009). This kinetic model was used and represented as;

$$\frac{t}{q_t} = \frac{1}{kq_e^2} + \frac{t}{q_e} \tag{6}$$

where q_e and q_t show the dye adsorbed on the adsorbent (mg g^{-1}) at equilibrium and at time t (min). k is the pseudo second-order rate constant of the sorption. Values of q_e and k were obtained from Eq. (6).

Recently, use of ANN has attracted much attention for process modeling to predict behavior of a system and to design a new process (Khataee and Kasiri, 2010; Cavasa et al., 2011; Çelekli and Geyik, 2011; Khataee et al., 2011; Yang et al., 2011). A three-layer ANN was used in this work (Fig. 6). The input layer had three neurons as initial pH value, initial dye concentration, and contact time. The output layer had one neuron as amount of *LR G* adsorbed on *WH*. A series of topologies was used to determine the optimum number of hidden nodes, in which the number of nodes was varied from 2 to 25. The number of neurons in the hidden layer had been selected as 20 neurons because of its minimum error values (%) for training and testing sets. Each topology was repeated three times to avoid random correlation due to random initialization of the weights.

The mean square error (*MSE*) was used as the error function:

$$MSE = \frac{1}{N}\sum_{i=1}^{n}(q_{predict} - q_{\exp})^2 \tag{7}$$

where N is the number of data point, $q_{predict}$ is the predicted sorption data from ANN and pseudo second models, q_{exp} is the observed experimental sorption data.

Regression analyses were carried out to compare experimental (q_{exp}) and predicted ($q_{predict}$) data from ANN and pseudo second kinetic models and their results are given in Fig. 7a and b, respectively. Determination of coefficients was found to be 0.998 and 0.992 for ANN and pseudo second models, respectively. ANN was found to be better model than that of pseudo second order kinetic model to describe sorption process within experimental ranges. Çelekli and Geyik (2011), Khataee et al. (2011), and Yang et al. (2011) observed similar results that ANN had well-fitting results to describe the experimental data.

Parameters obtained from ANN and pseudo second-order kinetic models are given in Table 1. The sorption of *LR G* on WH as function of contact time and initial dye concentrations at pH 1 with predicted data from ANN and pseudo second models are shown in Fig. 8a and b, respectively. Likely, both models had well-fitting to experimental data. However, according to values of determination of coefficient ($R^2 \geqslant 0.995$) and *MSE* (0.4993–5.0057), the ANN was found to be more suitable model to describe the sorption of *LR G* on the *WH*. Moreover, predicted q_t values from the ANN agreed very well with the experimental q_t values than those of pseudo second kinetic model. Similar results also observed in previous studies (Çelekli and Geyik, 2011; Khataee et al., 2011; Yang et al., 2011) that ANN had been shown well-fitting results to describe the experimental data.

Neural net weight matrix (Khataee and Kasiri, 2010) was used in order to assess the relative importance of the various operating (input) variables on the output variables. Results indicated that pH was the most efficient parameter (43%), followed by initial dye concentration (40%) for the sorption of *LR G* on *WH*. Similar results also observed in previous studies (Khataee et al., 2010; Çelekli and Geyik, 2011; Yang et al., 2011). Yang et al. (2011) reported that initial dye concentration was found to be the most important factor, followed by pH. Khataee et al. (2011) observed that the most important factor is the reaction time, followed by pH.

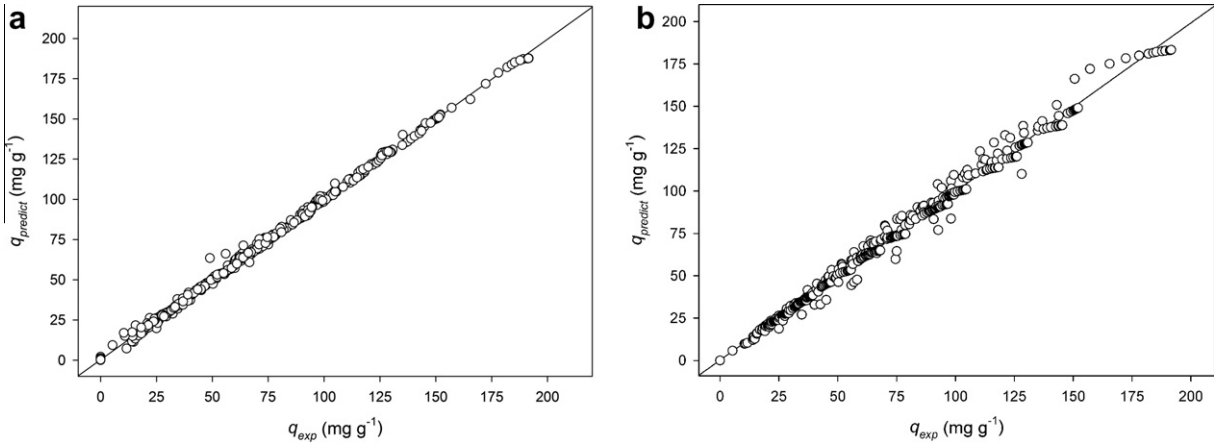

Fig. 7. Regression of the experimental data with those predicted data from: (a) ANN and (b) pseudo kinetic models (pH_i = 1–4, C_o = 50–800 mg L^{-1}, and t = 0–360 min).

Table 1
Kinetic parameters for the sorption of *LR G* on *WH* (pH_i 1, particle size = 125–250 μm, C_o = 50–800 mg L^{-1}, M = 1 g L^{-1}, and t = 0–360 min).

	C_o (mg L^{-1})	50	100	200	400	600	800
ANN	q_{exp}	36.76	67.35	100.89	129.58	151.38	187.74
	$q_{predict}$	38.48	67.17	100.01	129.31	150.98	186.40
	R^2	0.995	0.996	0.998	0.998	0.999	0.998
	MSE	0.4993	1.2504	1.3067	2.0387	1.807	5.0057
Pseudo second	$q_{predict}$	36.08	65.95	102.77	129.59	150.72	185.07
	R^2	0.984	0.970	0.974	0.990	0.974	0.963
	MSE	1.2956	8.0492	17.0451	9.1594	34.3554	75.1481

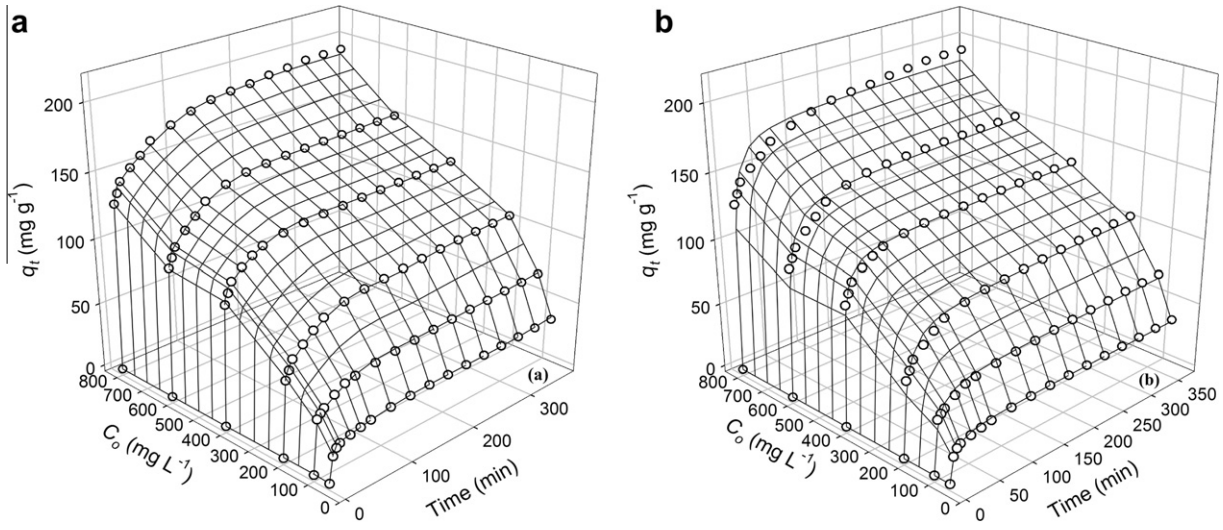

Fig. 8. Comparison of the experimental data with those predicted data from: (a) ANN and (b) pseudo second kinetic models (pH_i = 1, particle size = 125–250 μm, M = 1 g L^{-1}, C_o = 50–800 mg L^{-1}, and t = 0–360 min).

4. Conclusions

Results revealed that *WH* had a great potential to remove *LR G* from aqueous solution at different initial pH values, dye concentrations, and contact time. ANN was found to be excellent model because of lower *SME* and higher determination of coefficient values between the network prediction and corresponding experimental data. Results of this model showed that pH was the most efficient parameter (43%), followed by initial dye concentration (40%) for the sorption process. As a result, ANN model can be used in design and scale-up for removing of *LR G* on the *WH*.

Acknowledgements

Authors thank to Scientific Research Projects Executive Council of University of Gaziantep, DPT (T.R. Prime Ministry State Planning Organization) and also thank to Dr. Bülent Belibağlı for his comment.

References

Arief, V.O., Trilestari, K., Sunarso, J., Indraswati, N., Ismadji, S., 2008. Recent progress on biosorption of heavy metals from liquids using low cost biosorbents: characterization, biosorption parameters and mechanism studies: a review. Clean 36, 937–962.

Balci, B., Keskinkan, O., Avcı, M., 2011. Use of BDST and an ANN model for prediction of dye adsorption efficiency of Eucalyptus camaldulensis barks in fixed-bed system. Expert Syst. Appl. 38, 949–956.

Cardoso, N.F., Lima, E.C., Pinto, I.S., Amavisca, C.V., Royer, B., Pinto, R.B., Alencar, W.S., Pereira, S.F.P., 2011. Application of cupuassu shell as biosorbent for the removal of textile dyes from aqueous solution. J. Environ. Manage. 92, 1237–1247.

Cavasa, L., Karabaya, Z., Alyuruka, H., Doğan, H., Demir, G.K., 2011. Thomas and artificial neural network models for the fixed-bed adsorption of methylene blue by a beach waste *Posidonia oceanica* (L.) dead leaves. Chem. Eng. J. 171, 557–562.

Chowdhury, S., Chakraborty, S., Saha, P., 2011a. Biosorption of Basic Green 4 from aqueous solution by *Ananas comosus* (pineapple) leaf powder. Colloids Surf. B 84, 520–527.

Chowdhury, S., Mishra, R., Saha, P., Kushwaha, P., 2011b. Adsorption thermodynamics, kinetics and isosteric heat of adsorption of malachite green onto chemically modified rice husk. Desalination 265, 159–168.

Chowdhury, S., Saha, P., 2010. Sea shell powder as a new adsorbent to remove Basic Green 4 (Malachite Green) from aqueous solutions: equilibrium, kinetic and thermodynamic studies. Chem. Eng. J. 164, 168–177.

Çelekli, A., Yavuzatmaca, M., Bozkurt, H., 2010a. Modelling for removing of reactive red 120 on pistachio husk. Clean 38, 173–180.

Çelekli, A., Yavuzatmaca, M., Bozkurt, H., 2010b. An ecofriendly process: predictive modelling of copper adsorption from aqueous solution on *Spirulina platensis*. J. Hazard. Mater. 173, 123–129.

Çelekli, A., Geyik, F., 2011. Artificial Neural Networks (ANN) approach for modeling of removal of Lanaset Red G on *Chara contraria*. Bioresour. Technol. 102, 5634–5638.

Çelekli, A., Tanrıverdi, B., Bozkurt, H., 2011. Predictive modeling of removal of Lanaset Red G on *Chara contraria*; kinetic, equilibrium, and thermodynamic studies. Chem. Eng. J. 169, 166–172.

Doğan, M., Abak, H., Alkan, M., 2009. Adsorption of methylene blue onto hazelnut shell: kinetics, mechanism and activation parameters. J. Hazard. Mater. 164, 172–181.

Dutta, S., Parsons, S.A., Bhattacharjee, C., Bandhyopadhyay, S., Data, S., 2010. Development of an artificial neural network model for adsorption and photocatalysis of reactive dye on TiO2 surface. Expert Syst. Appl. 37, 8634–8638.

Gao, J., Zhang, Q., Su, K., Chen, R., Peng, Y., 2010. Biosorption of Acid Yellow 17 from aqueous solution by non-living aerobic granular sludge. J. Hazard. Mater. 174, 215–225.

Gupta, V.K., Jain, R., Shrivastava, M., 2010. Adsorptive removal of Cyanosine from waste water using coconut husks. J. Colloid Interf. Sci. 347, 309–314.

Ho, Y.S., McKay, G., 1999. Pseudo second-order model for sorption processes. Process Biochem. 34, 451–465.

Khataee, A.R., Kasiri, M.B., 2010. Artificial neural networks modeling of contaminated water treatment processes by homogeneous and heterogeneous nanocatalysis. J. Mol. Catal. A-Chem. 331, 86–100.

Khataee, A.R., Dehghan, G., Ebadi, A., Zarei, M., Pourhassan, M., 2010. Biological treatment of a dye solution by macroalgae *Chara sp.*: effect of operational parameters, intermediates identification and artificial neural network modeling. Bioresour. Technol. 101, 2252–2258.

Khataee, A.R., Dehghan, G., Zarei, M., Ebadi, A., Pourhassan, M., 2011. Neural network modeling of biotreatment of triphenylmethane dye solution by a green macroalgae. Chem. Eng. Res. Des. 89, 172–178.

Kumar, K.V., Porkodi, K., 2007. Mass transfer, kinetics and equilibrium studies for he biosorption of methylene blue using *Paspalum notatum*. J. Hazard. Mater. 146, 214–226.

Kumar, K.V., Porkodi, K., 2009. Modelling the solid–liquid adsorption processes using artificial neural networks rained by pseudo second order kinetics. Chem. Eng. J. 148, 20–25.

Khorramfar, S., Mahmoodi, N.M., Arami, M., Gharanjig, K., 2010. Equilibrium and kinetic studies of the cationic dye removal capability of a novel biosorbent *Tamarindus indica* from textile wastewater. Color. Technol. 126, 261–268.

Mahmoodi, N.M., Arami, M., Bahrami, H., Khorramfar, S., 2010. Novel biosorbent (Canola hull): surface characterization and dye removal ability at different cationic dye concentrations. Desalination 264, 134–142.

Mahmoodi, N.M., Arami, M., Bahrami, H., Khorramfar, S., 2011a. The effect of pH on the removal of anionic dyes from colored textile wastewater using a biosorbent. J. Appl. Polym. Sci. 120, 2996–3003.

Mahmoodi, N.M., Hayati, B., Arami, M., Lan, C., 2011b. Adsorption of textile dyes on Pine Cone from colored wastewater: kinetic, equilibrium and thermodynamic studies. Desalination 268, 117–125.

Muradoğlu, F., Oguz, H.I., Yıldız, K., Yilmaz, H., 2010. Some chemical composition of walnut (*Juglans regia* L.) selections from Eastern Turkey. Afr. J. Agricult. Res. 5 (17), 2379–2385.

Mui, E.L.K., Cheung, W.H., Valix, M., McKay, G., 2010. Dye adsorption onto char from bamboo. J. Hazard. Mater. 177, 1001–1005.

Plazinski, W., Rudzinski, W., Plazinska, A., 2009. Theoretical models of sorption kinetics including a surface reaction mechanism: a review. Adv. Colloid. Interface Sci. 152, 2–13.

Rafatullah, M., Sulaiman, O., Hashim, R., Ahmad, A., 2010. Adsorption of methylene blue on low-cost adsorbents: a review. J. Hazard. Mater. 177, 70–80.

Song, J., Zou, W., Bian, Y., Su, F., Han, R., 2011. Adsorption characteristics of methylene blue by peanut husk in batch and column modes. Desalination 265, 119–125.

Srinivasan, A., Viraraghavan, T., 2010. Decolorization of dye wastewaters by biosorbents: a review. J. Environ. Manage. 91, 1915–1929.

Wang, X.S., Li, Z.Z., Tao, S.R., 2009. Removal of chromium (VI) from aqueous solution using walnut hull. J. Environ. Manage. 90, 721–729.

Wang, L., Zhang, J., Zhao, R., Li, C., Li, Y., Zhang, C., 2010. Adsorption of basic dyes on activated carbon prepared from *Polygonum orientale* Linn: equilibrium, kinetic and thermodynamic studies. Desalination 254, 68–74.

WHO/UNICEF, 2000. Global Water Supply and Sanitation Assessment Report 2000. WHO, Geneva, 2000.

Xu, X., Gao, B.Y., Yue, Q.Y., Zhong, Q.Q., 2010. Preparation and utilization of wheat straw bearing amine groups for the sorption of acid and reactive dyes from aqueous solutions. J. Hazard. Mater. 182, 1–9.

Yang, J., Qiu, K., 2010. Preparation of activated carbons from walnut shells via vacuum chemical activation and their application for methylene blue removal. Chem. Eng. J. 165, 209–217.

Yang, Y., Wang, G., Wang, B., Li, Z., Jia, X., Zhou, Q., Zhao, Y., 2011. Biosorption of Acid Black 172 and Congo Red from aqueous solution by nonviable *Penicillium* YW 01: kinetic study, equilibrium isotherm and artificial neural network modeling. Bioresour. Technol. 102, 828–834.